

## A data-driven methodology for cross-visit sub-segmentation of tumours in DCE-MRI studies

G. A. Buonaccorsi<sup>1</sup>, J. P. O'Connor<sup>1,2</sup>, C. J. Rose<sup>1</sup>, C. Roberts<sup>1</sup>, A. Counce<sup>1</sup>, S. Cheung<sup>1</sup>, Y. Watson<sup>1</sup>, K. Davies<sup>1</sup>, L. Hope<sup>2</sup>, A. Jackson<sup>1</sup>, G. C. Jayson<sup>2</sup>, and G. J. Parker<sup>1</sup>

<sup>1</sup>ISBE, University of Manchester, Manchester, United Kingdom, <sup>2</sup>CRUK Dept of Medical Oncology, Christie Hospital, Manchester, United Kingdom

**Introduction** It is common in quantitative dynamic contrast enhanced MRI (DCE-MRI) to acquire volume images at regular time intervals and then apply voxel-by-voxel model-based<sup>1</sup> and/or model-free<sup>2</sup> methods to analyse the time series data. This practice requires the assumption that the microvascular structure and physiology of the tissues that correspond to any given voxel will determine the characteristics of the time series data for that voxel, e.g. average signal intensity and time series curve shape, which will in turn determine the values of the estimated parameters, e.g. IAUC,  $K^{trans}$ ,  $v_e$  and  $v_p$ . It is a small step to hypothesize that if the voxels in an image are subjected to a classification (i.e. segmentation) based on the characteristics of the time series data then that classification will be meaningful in terms of the underlying microvascular structure and function. For multi-visit studies, we further assume that this holds for images acquired at different visits and a cross-visit segmentation will therefore allow us to follow visit-by-visit changes in the size and location of regions of a tumour with distinct physiological characteristics. On this basis, we describe a data-driven image segmentation method for use with DCE-MRI time series data.

**Data** All patients in our study had primary ovarian cancer and had received conventional treatment using cytotoxic agents. To follow the progression of residual disease in the abdomen and pelvis, we performed DCE-MRI at monthly intervals for six-months or until further treatment was required. At each visit we acquired 75 dynamic 3D spoiled gradient echo (Fast Field Echo – FFE) images with a temporal resolution of 4.96 s, voxel size of 2.93 x 2.93 x 4.0 mm<sup>3</sup> and FOV of 375 x 375 x 100 mm<sup>3</sup> on a Philips 1.5 T Intera scanner. We manually defined tumour volumes of interest (VOI) in 3D on co-localised T<sub>1</sub>- and T<sub>2</sub>-weighted image volumes.

**Methods** We converted the DCE-MRI signal intensity data to contrast agent concentrations to remove inter-visit differences in FFE signal intensity due to variations in scanner gain, etc. Then we extracted the entire contrast agent concentration time series for each voxel in the tumour VOI and for each visit into a single cross-visit data matrix. We reduced the data dimensionality using principal components analysis<sup>3</sup> (PCA) in Matlab<sup>®</sup>, retaining the principal components indicated by the log-eigenvalue plots<sup>3</sup>. Next we performed k-means clustering<sup>4</sup> (also in Matlab<sup>®</sup>) using multiple start points and multiple numbers of clusters, retaining the solution that minimised the sum of the squared euclidean distance from each data point to its assigned cluster mean. Finally, we generated segmentation images from the clustering results and used the cluster VOIs to calculate cluster size and per-cluster statistics from 3D maps of  $K^{trans}$ ,  $v_e$  and  $v_p$  which we obtained for each visit by fitting the extended Kety model<sup>5</sup> using the locally-written MaDyM package.

**Results** Figure 1 shows examples of single voxel DCE-MRI time series curves with very different characteristics. Figure 2 shows the segmentation we obtained for a typical patient data set — the clusters have consistent colour-mapping across the 6 visits. When the cluster VOIs were applied to parameter maps from extended Kety modelling for the same patient, we obtained the trends shown in the graphs of Fig. 3. In general the differences in parameter values were not statistically significant. Note that the line colours for Figs. 1 and 3 correspond to the cluster colours in Fig. 2.

**Discussion** In Fig. 1, the voxel time series curve from Cluster 1 (blue) shows that no significant contrast enhancement occurred in the corresponding tissue; Cluster 2 (green) shows significant enhancement with a clear first-pass peak and Cluster 4 (red) shows intermediate enhancement. We selected the voxels retrospectively, to illustrate the principle behind our methodology, and we would expect any useful classification algorithm to place them in distinct classes. Nevertheless, it is encouraging that the classification was not obscured after dimensionality reduction with PCA.

Radiological observations based on the higher resolution T<sub>1</sub>- and T<sub>2</sub>-weighted image volumes established that the tumour in this data set had a cystic component, which reduced in volume as the study progressed and was displaced by new tumour mass. The location of the cyst matched that of Cluster 1, which also reduced in size over the period of the study (Fig. 3): this cluster showed low enhancement (Fig. 1), and had very low values of all extended Kety model parameters (Fig. 3). We believe it is reasonable to conclude that Cluster 1 corresponds to the cystic component.

While we do not have independent information, radiological or otherwise, that would allow us to deduce which tissue types comprise Clusters 2 to 4, it is not necessary to do so. Each cluster is likely to be heterogeneous within itself, although we expect intra-cluster heterogeneity to be lesser than inter-cluster heterogeneity. Figure 3 provides some evidence to support this assertion. While the differences between median cluster VOI parameter values are not statistically significant, clear trends may be observed. All extended Kety model parameters tend to be lower for Cluster 4 than for Clusters 2 and 3, while Cluster 3 tends to have higher  $K^{trans}$  and  $v_p$  but lower  $v_e$  than Cluster 2. Typical clinical DCE-MRI studies (e.g. of treatment response to anti-angiogenic or vascular-disrupting agents) report parameter statistics averaged over the whole tumour VOI<sup>6</sup>. However, it is likely that different tumour sub-compartments will respond differently to treatment. Our cross-visit segmentation method may allow us to follow the evolution of sub-compartments of tumours throughout a DCE-MRI study and to observe changes in response to treatment including the appearance of new sub-compartments or the disappearance of old ones.

**Conclusions** We have described an unsupervised, data-driven method of cross-visit image segmentation for DCE-MRI time series data and illustrated its application in a clinical setting. The method is modular and could be refined, e.g. by replacing the k-means clustering with a more flexible fuzzy clustering such as c-means. We believe that it will provide an objective means of following the visit-by-visit evolution of tumour sub-compartments with distinct physiological characteristics in clinical studies using DCE-MRI.

**References** 1. Parker GJM and Buckley DL in Jackson A, Buckley DL, Parker GJM (eds.) *Dynamic contrast-enhanced magnetic resonance imaging in oncology*. Springer, Berlin (2005). 2. Evelhoch JL, LoRusso PM, *et al.* Clin Cancer Res **10**: 3650–3657, 2004. 3. Jolliffe IT. *Principal Components Analysis*. Springer, New York (2002). 4. Everitt BS. *Cluster Analysis*. Edward Arnold, London (1993). 5. Tofts PS. *J Magn Reson Imag* **7**: 91-101, 1997. 6. Liu G, Rugo HS, *et al.* J. Clin. Oncol. **23**: 5464-5473, 2005.

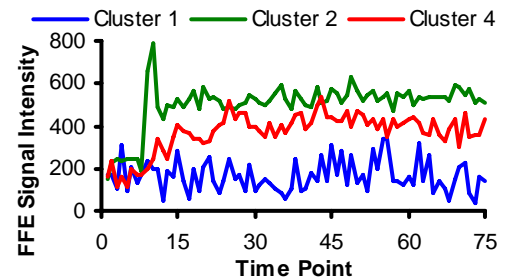


**Figure 1** Single-voxel time-series data for 3 locations in the same tumour (colours match the corresponding clusters in Fig. 2).

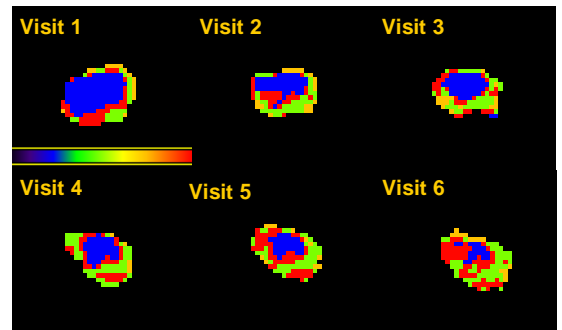


**Figure 2** Four-cluster segmentation of a tumour across six visits (no treatment or other intervention between visits).

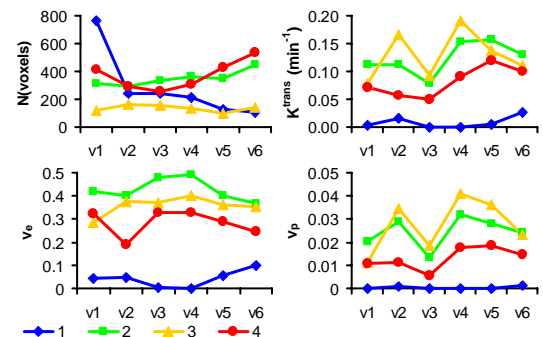


**Figure 3** Number of voxels and median Kety model parameter values (colours match the corresponding clusters in Fig. 2).